

Refractive index of quark-gluon plasma: Kinetic theory with a Bhatnagar-Gross-Krook collisional kernel

Bing-feng Jiang,^{1,*} De-fu Hou,^{2,†} and Jia-rong Li^{2,‡}

¹*Center for Theoretical Physics and School of Sciences, Hubei University for Nationalities, Enshi, Hubei 445000, China*

²*Key Laboratory of Quark and Lepton Physics (MOE) and Institute of Particle Physics, Central China Normal University, Wuhan, Hubei 430079, China*

(Received 8 September 2016; published 19 October 2016)

We derive the electric permittivity ϵ and magnetic permeability μ_M of the quark-gluon plasma (QGP) with the kinetic theory associated with a Bhatnagar-Gross-Krook (BGK) collisional kernel. Based on them, we study the effect of collisions on the refractive index of QGP. Compared to the collisionless case, collisions change the ω -behavior of ϵ and μ_M dramatically, which is responsible for the fact that the real and imaginary parts of n^2 and the Depine-Lakhtakia index n_{DL} are smooth functions of ω . For a small collision rate ν , the Depine-Lakhtakia index n_{DL} is negative in some frequency range. When the collision rate increases, the frequency range for $n_{DL} < 0$ becomes narrower. Numerical results show a critical collision rate $\nu \sim 0.2m_D$, above which the Depine-Lakhtakia index n_{DL} is positive for all frequency regions, which indicates a normal refractive index. In contrast to the collisionless case, there exists some frequency range in which $n_{DL} < 0$ and the propagating mode may satisfy the dispersion relation $n^2\omega^2 = k^2$ simultaneously, which implies the existence of a negative refractive index.

DOI: 10.1103/PhysRevD.94.074026

I. INTRODUCTION

Quark-gluon plasma (QGP) is a special state of matter that is believed to be produced in ultrarelativistic heavy-ion collisions with an energy density above 1 GeV/fm³ in ground laboratories. The initial energy density that the Relativistic Heavy-Ion Collider (RHIC) and the Large Hadron Collider (LHC) can achieve is much higher than that [1]. One striking finding at the RHIC is that the produced hot quantum chromodynamics (QCD) plasma in heavy-ion collisions behaves as a nearly perfect fluid with a small viscosity [2–5]. The first results from the LHC also qualitatively support the similar conclusion drawn at the RHIC [6,7]. The study of QGP properties has attracted intense interest in recent years.

Electromagnetic probes, once produced in heavy-ion collisions, will be not involved in strong interactions and pass through the medium almost undisturbed. So electromagnetic probes, carrying information directly from wherever they were generated, may be clear and promising signatures for QGP in relativistic heavy-ion collisions. At the very early stage of relativistic heavy-ion collisions, named the glasma stage [8], and at the late stage of the evolution process in the near T_c region in the so-called magnetic scenario for QGP [9,10], there are color-electric flux tubes that contain strong color-electric fields. On the other hand, it has been argued that the very strong magnetic

fields will be produced perpendicular to the reaction plane in off-central heavy-ion collisions [11–14]. Electromagnetic properties will play an important role in the evolution of hot QCD matter produced in heavy-ion collisions and many heavy-ion phenomena may be relevant to them. Therefore, the study of them may be helpful for understanding the nature of QGP.

The refractive index reflects the propagation property of light in an electromagnetic medium, which is one of the most important electromagnetic properties in a medium. It can be determined in terms of electric permittivity $\epsilon(\omega, k)$ (EP) and magnetic permeability $\mu_M(\omega, k)$ (MP). A gluon is the QCD counterpart of a photon. In addition, jet quenching has been proposed as a potential signal for QGP and has become an active field in heavy-ion collisions in the last three decades, which is relevant to the parton propagation in the hot medium. So the study of the refraction index in QGP may be helpful to understand the nature of QGP.

Amariti *et al.* have studied the refractive index of the strongly coupled system with the string-inspired theory of AdS/CFT correspondence in Ref. [15]. Along that line, some investigations on refractive properties have been carried out in strongly coupled and correlation systems in the past years [16–23]. Recently, Juan Liu *et al.* have extended the study of the refractive index of light to the weakly coupled QGP within the framework of the hard thermal loop perturbation theory [24]. Bing-feng Jiang *et al.* have studied the refractive index of viscous QGP [25] subsequently within the framework of viscous chromohydrodynamics [26]. In addition, the viscous effect on electromagnetic properties in a charged fluid system has

*jiangbf@mails.ccnucnu.edu.cn

†houdf@mail.ccnucnu.edu.cn

‡ljr@mail.ccnucnu.edu.cn

also been addressed in recent literature [27]. Later, authors have studied the electric permittivity, magnetic permeability, and refractive index in a relativistic electron gas with quantum electrodynamics at finite temperature and density [28]. In the present paper, we will study the refractive index of QGP within the framework of the transport approach associated with a Bhatnagar-Gross-Krook (BGK) collisional kernel.

Collisions are one of the main sources of dissipation. For a long time, the BGK collisional kernel has been proposed in the Boltzmann transport theory to study the plasma properties in an electromagnetic plasma [29]. It should be noted that the derivation of the collisional terms of the transport equations for the QCD plasma has been a complex task and is far from strictly solved [30–33]. Carrington *et al.* have extended the study of kinetic theory with a BGK-type collisional kernel to the QGP system, and they investigated the dielectric functions and the dispersion relations in Ref. [34]. Then the plasma collective modes in QGP were investigated, including the effect of BGK collisions with an anisotropic momentum distribution [35]. It was found that collisions strongly affect QGP unstable modes, which may speed up the thermalization process of the QCD plasma produced in heavy-ion collisions at the RHIC. In addition, the collision effect on the wakes caused by a fast parton traveling through QGP have been addressed recently [36,37].

In the present paper, we will derive the gluon polarization tensor by solving the kinetic equations associated with a BGK-type collisional kernel. The electric permittivity $\epsilon(\omega, k)$ and magnetic permeability $\mu_M(\omega, k)$ are evaluated from the obtained gluon polarization tensor, through which the refractive index is investigated subsequently. Through the polarization tensor, electric permittivity, and magnetic permeability, the collision effect is encoded into the refractive index. Thus we can study its effect on the latter. It should be noted that we are going to study the chromodynamic properties of QGP here—we should add the prefix “chromo” to the electromagnetic quantities of QGP, such as chromoelectric permittivity, chromomagnetic permeability, and chromorefractive index. For concision, we will omit that prefix in the following, but we should bear in mind that what we want to study are the chromodynamic quantities.

The paper is organized as follows. In Sec. II, we will briefly review the formulism of the electromagnetic properties in an electromagnetic plasma, which can be applied to the QGP system. In Sec. III, we will make a brief derivation of the polarization tensor and the electric permittivity and the magnetic permeability subsequently by solving the kinetic equations with the BGK collisional term. We will give numerical results of the electric permittivity, magnetic permeability, and the refractive index and we discuss the collision’s effect on them in Sec. IV. In Sec. V we will give a summary.

The natural units $k_B = \hbar = c = 1$; the metric $g_{\mu\nu} = (+, -, -, -)$; and the notations $K = (\omega, \mathbf{k})$, $k = |\mathbf{k}|$ are used in the paper.

II. ELECTROMAGNETIC PROPERTIES IN PLASMA

In this section, by following the classical literature [38], we will give a brief derivation of the electromagnetic properties in a homogeneous and isotropic plasma. Some details can be also found in the literature [24,25,39]. In addition, the extension of the discussion to an anisotropic medium has been addressed in Ref. [24].

Usually a pair of four-vectors \tilde{E}^μ , \tilde{B}^μ are introduced to covariantly describe the electric and magnetic properties in plasma,

$$\tilde{E}^\mu = u_\nu F^{\nu\mu}, \quad \tilde{B}^\mu = \frac{1}{2} \epsilon^{\nu\lambda\rho\mu} F_{\nu\lambda} u_\rho, \quad (1)$$

where u^ν is the fluid four-velocity and $F^{\mu\nu}$ is constructed as

$$F^{\mu\nu} = u^\mu \tilde{E}^\nu - \tilde{E}^\mu u^\nu + \epsilon^{\mu\nu\lambda\rho} \tilde{B}_\lambda u_\rho. \quad (2)$$

In Eqs. (1)–(2), one should not confuse the greek index μ with the magnetic permeability μ_M mentioned in the Introduction. The free action can be expressed in terms of the Fourier-transformed \tilde{E}^μ , \tilde{B}^μ :

$$S_0 = -\frac{1}{2} \int \frac{d^4 K}{(2\pi)^4} \{ \tilde{E}^\mu(K) \tilde{E}_\mu(-K) - \tilde{B}^\mu(K) \tilde{B}_\mu(-K) \}. \quad (3)$$

When interactions between the constituents of plasma are taken into account, the correction to the action is

$$S_{\text{int}} = -\frac{1}{2} \int \frac{d^4 K}{(2\pi)^4} A^\mu(-K) \Pi_{\mu\nu}(K) A^\nu(K), \quad (4)$$

where the terms that are cubic and higher order in $A^\mu(K)$ are omitted. In Eq. (4), $A^\mu(K)$ is a vector field in momentum space, and $\Pi_{\mu\nu}(K)$ is the polarization tensor that embodies the medium effects in plasma. In a homogeneous and isotropic medium, the polarization tensor can be divided into longitudinal and transverse parts

$$\Pi_{\mu\nu}(K) = \Pi_L(K) P_{\mu\nu}^L(K) + \Pi_T(K) P_{\mu\nu}^T(K) \quad (5)$$

with projectors defined as $P_{00}^T = P_{0i}^T = P_{i0}^T = 0$, $P_{ij}^T = \delta^{ij} - \frac{k^i k^j}{k^2}$, $P_{\mu\nu}^L = \frac{k^\mu k^\nu}{K^2} - g^{\mu\nu} - P_{\mu\nu}^T$ [40,41]. Thus, the effective action, including medium effects, is

$$S_{\text{eff}} = S_0 + S_{\text{int}}, \quad (6)$$

which also can be described as

$$S_{\text{eff}} = -\frac{1}{2} \int \frac{d^4 K}{(2\pi)^4} \left[\epsilon \tilde{E}^\mu(K) \tilde{E}_\mu(-K) - \frac{1}{\mu_M} \tilde{B}^\mu(K) \tilde{B}_\mu(-K) \right]. \quad (7)$$

In (7), ϵ and μ_M are the electric permittivity and magnetic permeability mentioned in the Introduction, which can describe the difference between the electric and magnetic properties of the vector field in the medium and those in the vacuum. According to Eqs. (3), (4), and (7), one can get the electric permittivity and magnetic permeability in plasma as follows:

$$\epsilon(\omega, k) = 1 - \frac{\Pi_L(\omega, k)}{K^2}, \quad (8)$$

$$\frac{1}{\mu_M(\omega, k)} = 1 + \frac{K^2 \Pi_T(\omega, k) - \omega^2 \Pi_L(\omega, k)}{k^2 K^2}. \quad (9)$$

The refraction index is defined in terms of the electric permittivity and magnetic permeability as

$$n^2 = \epsilon(\omega, k) \mu_M(\omega, k), \quad (10)$$

which is a square definition and not sensitive to the simultaneous change of signs of ϵ and μ_M . About 50 years ago, Veselago proposed that the simultaneous change from positive ϵ and μ_M to negative $-\epsilon$ and $-\mu_M$ corresponds to the transformation of the refractive index from one branch, $n = \sqrt{\epsilon(\omega, k) \mu_M(\omega, k)}$, to the other, $n = -\sqrt{\epsilon(\omega, k) \mu_M(\omega, k)}$, i.e., the change from a general refractive index to a negative one [42]. The physical nature of the negative refraction is that the electromagnetic phase velocity propagates opposite to the energy flow [42–44]. Nevertheless, no natural material shows such special properties (recently some people argued that the relativistic electron gas may be one of nature's candidates for the realization of a negative refraction system [28]). Around 2000, by manipulating the array of small and closely spaced elements, scientists have constructed a negative refraction material in the laboratory [45,46]. Since then, the study of negative refraction has attracted intense interest. It has been found that negative refraction is a general phenomenon for a charged fluid system in some frequency region [17].

The criterion for negative refraction is $\epsilon < 0$ and $\mu_M < 0$ simultaneously for the real electric permittivity and magnetic permeability medium. If dissipation is taken into account, the situation is complicated. The electric permittivity and magnetic permeability are generally complex-valued functions of ω and k , such as $\epsilon(\omega, k) = \epsilon_r(\omega, k) + i\epsilon_i(\omega, k)$, $\mu_M(\omega, k) = \mu_r(\omega, k) + i\mu_i(\omega, k)$, so is the refractive index n . According to the phase velocity propagating antiparallel to the energy flow, some authors have derived the condition for negative refraction in a

dissipative medium and found that it is not necessary for $\epsilon_r < 0$ and $\mu_r < 0$ simultaneously [47]. Later, another simple, convenient, and widely adopted condition was derived as [48]

$$n_{\text{DL}} = \epsilon_r |\mu_M| + \mu_r |\epsilon| < 0, \quad (11)$$

where n_{DL} is called the Depine-Lakhtakia index. $n_{\text{DL}} < 0$ implies $\text{Re}n < 0$; otherwise we will have a normal refraction index [48].

III. ELECTRIC PERMITTIVITY AND MAGNETIC PERMEABILITY IN KINETIC THEORY: INCLUSION OF COLLISIONS

The transport equations for the quark, antiquark, and gluon can be expressed as equations for functions $f_a^i(p, X)$ with $i \in \{q, \bar{q}, g\}$ and $a = 1, 2, \dots, N_c^2 - 1$, which correlate to the corresponding phase space densities, i.e., Wigner functions [35,36,49]. In the case of linear approximation $f_a^i(p, X) = f^i(\mathbf{p}) + \delta f_a^i(p, X)$, the transport equations can be given as [35,36,49]

$$V \cdot \partial_X \delta f_a^i(p, X) + g \theta_i V_\mu F_a^{\mu\nu}(X) \partial_\nu^{(p)} f^i(\mathbf{p}) = C_a^i(p, X), \quad (12)$$

where $V = (1, \mathbf{v})$ with $\mathbf{v} = \mathbf{p}/|\mathbf{p}|$ and g is the strong coupling constant. $\theta_g = \theta_q = 1$, $\theta_{\bar{q}} = -1$, and $\partial_\nu^{(p)}$ denotes the four-momentum derivative. $F^{\mu\nu} = \partial^\mu A^\nu - \partial^\nu A^\mu - ig[A^\mu, A^\nu]$ represents the field strength tensor with the gauge field $A^\mu = A_a^\mu T^a$ or $A^\mu = A_a^\mu \tau^a$, where τ^a and T^a are the $\text{SU}(N_c)$ group generators in the fundamental and adjoint representations with $\text{Tr}[\tau^a, \tau^b] = \frac{1}{2} \delta^{ab}$, $\text{Tr}[T^a, T^b] = N_c \delta^{ab}$. $C_a^i(p, X)$ denotes the collision term. In the following consideration, we will adopt the BGK-type collisional term, given by [34,35]

$$C_a^i(p, X) = -\nu \left[f_a^i(p, X) - \frac{N_a^i(X)}{N_{\text{eq}}^i} f_{\text{eq}}^i(|\mathbf{p}|) \right]. \quad (13)$$

In Eq. (13), particle numbers $N_a^i(X)$ and N_{eq}^i read [34,35]

$$N_a^i(X) = \int_{\mathbf{p}} f_a^i(p, X), \quad N_{\text{eq}}^i = \int_{\mathbf{p}} f_{\text{eq}}^i(|\mathbf{p}|) = \int_{\mathbf{p}} f^i(\mathbf{p}), \quad (14)$$

$$\int_{\mathbf{p}} := \int \frac{d^3 p}{(2\pi)^3}.$$

In Eq. (13), ν denotes the collision rate, which implies that collisions equilibrate the system within a time interval proportional to ν^{-1} . As considered in Refs. [34,35], we will regard the collision rate ν as a free input parameter independent of momentum and particle species. When the ratio $N_a^i(X)$ over $N_{\text{eq}}^i(X)$ in the second term in Eq. (13)

is set to one, the collisional term changes to the familiar one in the relaxation time approximation. It is argued that the BGK collisional term is an improvement of the one in the relaxation time approximation for the transport equation. The advantage of the BGK collisional term is that it can conserve the particle numbers of system instantaneously [34,35].

The total induced color current due to the fluctuations of $\delta f_a^i(p, X)$ can be expressed as [35]

$$\delta f^i(p, K) = \frac{-ig\theta_i V_\mu F^{\mu\nu}(K) \partial_\nu^{(p)} f^i(\mathbf{p}) + i\nu f_{\text{eq}}^i(\mathbf{p}) (\int_{\mathbf{p}'} \delta f^i(p', K)) / N_{\text{eq}}}{\omega - \mathbf{v} \cdot \mathbf{k} + i\nu}, \quad (16)$$

where the color index is suppressed. The derivation of $\delta f_a^i(p, X)$ in the case of the anisotropic momentum distribution can be found in Appendix A in [35] and in Ref. [36]. Substituting the obtained $\delta f_a^i(p, K)$ from Eq. (16) into Eq. (15), one can get the induced color current. According to the relation $\Pi_{ab}^{\mu\nu} = \frac{\delta J_{\text{inda}}^{\mu\nu}(K)}{\delta A_a^\nu(K)}$ in the linear response theory, one can arrive at the polarization tensor [35,36]

$$\begin{aligned} \Pi_{ab}^{\mu\nu}(K) &= \delta_{ab} g^2 \int_{\mathbf{p}} V^\mu \partial_\beta^{(p)} f(\mathbf{p}) \mathcal{M}^{\gamma\beta}(K, V) D^{-1}(K, \mathbf{v}, \nu) \\ &+ \delta_{ab} i\nu g^2 \int \frac{d\Omega}{4\pi} V^\mu D^{-1}(K, \mathbf{v}, \nu) \\ &\times \int_{\mathbf{p}'} \partial_\beta^{(p')} f(\mathbf{p}') \mathcal{M}^{\gamma\beta}(K, V') \\ &\times D^{-1}(K, \mathbf{v}', \nu) \mathcal{W}^{-1}(K, \nu), \end{aligned} \quad (17)$$

with

$$\begin{aligned} \mathcal{M}_{\gamma\beta}(K, V) &:= g_{\gamma\beta}(\omega - \mathbf{k} \cdot \mathbf{v}) - V_\gamma K_\beta, \\ D^{-1}(K, \mathbf{v}, \nu) &:= \omega + i\nu - \mathbf{k} \cdot \mathbf{v}, \end{aligned} \quad (18)$$

and

$$\begin{aligned} \mathcal{W}(K, \nu) &:= 1 - i\nu \int \frac{d\Omega}{4\pi} D^{-1}(K, \mathbf{v}, \nu), \\ f(\mathbf{p}) &= 2N_c f^g(\mathbf{p}) + N_f [f^q(\mathbf{p}) + f^{\bar{q}}(\mathbf{p})]. \end{aligned} \quad (19)$$

We have briefly reviewed the derivation of the polarization tensor in QGP within the framework of kinetic theory associated with the BGK collisional term by following the pioneer work [34,35]. For details please refer to Refs. [34–36]. It is easy to test that Eq. (17) is diagonal in color and transverse, i.e., $K_\mu \Pi^{\mu\nu} = K_\nu \Pi^{\mu\nu}$.

In terms of Eqs. (8)–(9) and Eqs. (5), (17), one can arrive at the electric permittivity [34,37],

$$\begin{aligned} J_{\text{inda}}^\mu &= g \int_{\mathbf{p}} V^\mu \{ 2N_c \delta f_a^g(p, X) + N_f [\delta f_a^q(p, X) \\ &- \delta f_a^{\bar{q}}(p, X)] \}. \end{aligned} \quad (15)$$

Solving Eq. (12) associated with Eq. (13) and Fourier-transforming, one can get [34]

$$\begin{aligned} \epsilon(\omega, k) &= 1 + \frac{m_D^2}{k^2} \left(1 - \frac{\omega + i\nu}{2k} \ln \frac{\omega + i\nu + k}{\omega + i\nu - k} \right) \\ &\times \left(1 - \frac{i\nu}{2k} \ln \frac{\omega + i\nu + k}{\omega + i\nu - k} \right)^{-1}, \end{aligned} \quad (20)$$

and the magnetic permeability finally,

$$\mu_M(\omega, k) = \frac{1}{1 + \frac{\omega^2 m_D^2}{k^4} \left(1 - \frac{\omega z}{2k - i\nu k} + \frac{2\omega + 2i\nu + kz}{4\omega} - \frac{(\omega + i\nu)^2 z}{4\omega k} \right)}, \quad (21)$$

where $z = \ln \frac{\omega + i\nu + k}{\omega + i\nu - k}$ and m_D is the isotropic Debye mass denoted as $m_D^2 = -\frac{g^2}{2\pi^2} \int_0^\infty dp p^2 \frac{df(\mathbf{p})}{dp}$. A derivation of μ_M with more details can be found in Appendix A. Through the polarization tensor, the collision rate is encoded into the electric permittivity and magnetic permeability. Combined with Eqs. (20)–(21) and Eqs. (10)–(11), one can study the collision effect on the refractive index.

IV. COLLISION EFFECT ON THE REFRACTIVE INDEX: NUMERICAL ANALYSIS

We will apply the kinetic theory associated with the BGK collisional term to investigate the electric permittivity, magnetic permeability, and refractive index, which implies that the adopted theoretical framework is perturbative. The collision rate ν cannot be determined in that theoretical framework consistently. As in Refs. [34–37], we will regard the collision rate ν as an input parameter independent of ω and k to study its effect on those electromagnetic quantities. In the literature [35], Schenke *et al.* illuminated that the collision rate lies in the range $\nu \sim 0.1\text{--}0.2m_D$ for $\alpha_s = 0.2\text{--}0.4$ with a perturbative consideration for parton scatterings. In the present paper, we will study the collision effect on the electric permittivity, magnetic permeability, and refractive index for $\nu \in [0\text{--}0.3m_D]$. In addition, in numerical analysis, scales such as $k = 0.2m_D$ are used to study the ω behavior of the electromagnetic properties.

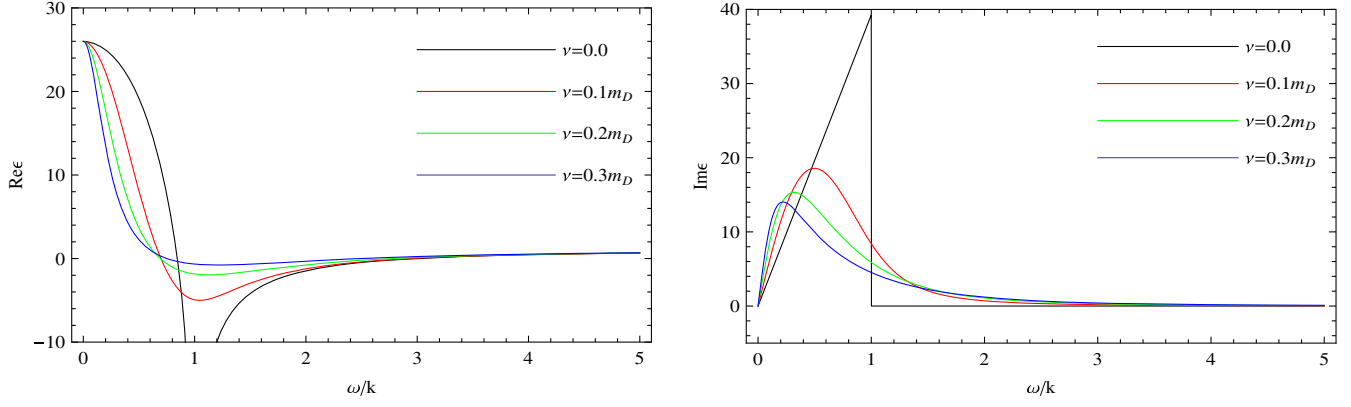


FIG. 1. The electric permittivity for different collision rates in units of m_D . Left panel: The real part. Right panel: The imaginary part. The black, red, green, and blue curves are for the cases of $\nu = 0, 0.1m_D, 0.2m_D, \text{ and } 0.3m_D$, respectively.

We present the numerical results of the real and imaginary parts of the electric permittivity and magnetic permeability for different collision rates in Figs. 1 and 2, respectively. When $\nu = 0$, ϵ and μ_M recover the corresponding results in the hard thermal loop approximation (HTLA) [24,25,30,34,35,38,40,41]. As shown by the black curves in the left panels in Figs. 1 and 2, the real parts of the electric permittivity and magnetic permeability show frequency poles at $\omega/k = 1$ and $\omega/k \sim 2$, respectively. On the other hand, ϵ and μ_M have nonzero imaginary parts due to the Landau damping in the frequency range $\omega/k \leq 1$. For $\omega/k > 1$, the corresponding imaginary parts turn to zero except for a frequency pole $\omega/k \sim 2$ for the magnetic permeability. While for $\nu > 0$, both the real and imaginary parts of the electric permittivity and magnetic permeability are smooth functions of ω and have no poles, as shown by the red, green, and blue curves in Figs. 1 and 2. In addition, both ϵ and μ_M gain a nonzero imaginary part even in the frequency region $\omega/k > 1$.

Carrington *et al.* mentioned that the collisional electric permittivity and magnetic permeability do not follow from the collisionless case by simply replacing ω by $\omega + i\nu$ [34].

In the following, as an example, we will give an investigation on the analysis structure of the collisional ϵ , which will shed light on the collision effect on the electromagnetic quantities. We firstly focus on the logarithmic function $\ln \frac{\omega+k+i\nu}{\omega-k+i\nu} = a + bi$, where a, b are real functions of ω, k , and ν . After some algebra, the logarithmic function can be written as

$$\begin{aligned} \ln \frac{\omega+k+i\nu}{\omega-k+i\nu} &= \ln \frac{(\omega+k+i\nu)(\omega-k-i\nu)}{(\omega-k)^2 + \nu^2} \\ &= \ln R - i\theta, \end{aligned} \quad (22)$$

with

$$\begin{aligned} a = \ln R, \quad b = -\theta, \quad R &= \frac{\sqrt{(\omega^2 - k^2 + \nu^2)^2 + 4k^2\nu^2}}{(\omega-k)^2 + \nu^2}, \\ \theta &= \arccos \frac{(\omega^2 - k^2 + \nu^2)}{\sqrt{(\omega^2 - k^2 + \nu^2)^2 + 4k^2\nu^2}}. \end{aligned} \quad (23)$$

For a detailed derivation, please refer to Appendix B.

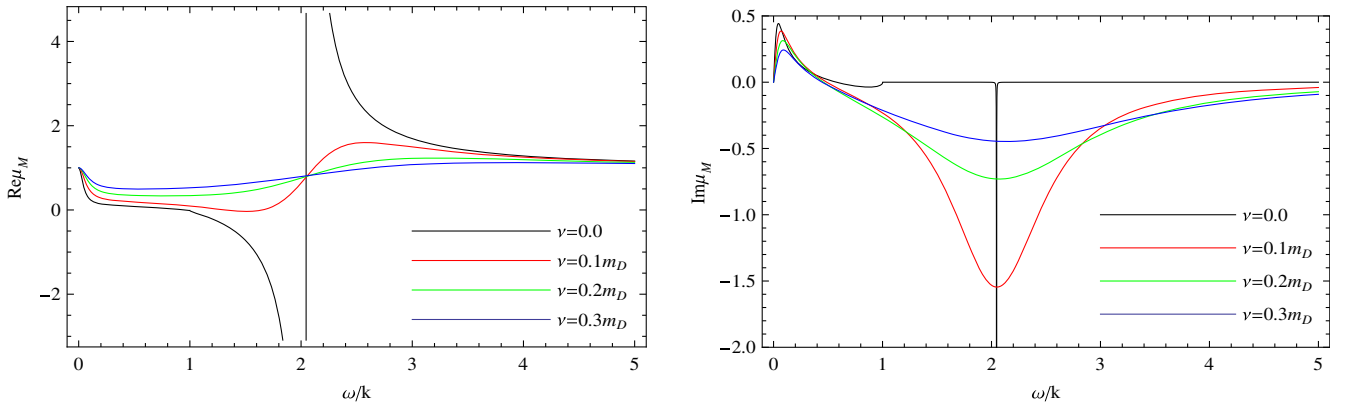


FIG. 2. The magnetic permeability for different collision rates in units of m_D . Left panel: The real part. Right panel: The imaginary part. The black, red, green, and blue curves are for the cases of $\nu = 0, 0.1m_D, 0.2m_D, \text{ and } 0.3m_D$, respectively.

By substituting (22) into (20), we can obtain the real and imaginary parts of the electric permittivity as follows (for details please refer to Appendix C):

$$\text{Re}\epsilon(\omega, k) = 1 + \frac{m_D^2}{k^2} \cdot \left\{ 1 - \frac{2\omega k \ln R}{4k^2 + \nu^2(\theta^2 + \ln^2 R) - 4k\nu\theta} \right\}, \quad (24)$$

$$\text{Im}\epsilon(\omega, k) = -\frac{m_D^2}{k^2} \cdot \frac{\omega\nu(\theta^2 + \ln^2 R) - 2\omega k\theta}{4k^2 + \nu^2(\theta^2 + \ln^2 R) - 4k\nu\theta}, \quad (25)$$

which coincide with the results in [37] and in [36] in the collisional isotropic case ($\nu \neq 0$, $\xi = 0$).

When $\nu = 0$, in terms of the logarithmic function derived in Appendix B,

$$\ln \frac{\omega + k + i0^+}{\omega - k + i0^+} = \ln \left| \frac{\omega + k}{\omega - k} \right| - i\pi\Theta(k^2 - \omega^2), \quad (26)$$

the electric permittivity (20) turns to the well-known result in the HTLA [30,38,40,41,49]:

$$\epsilon(\omega, k) = 1 + \frac{m_D^2}{k^2} \left(1 - \frac{\omega}{2k} \cdot \left(\ln \left| \frac{\omega + k}{\omega - k} \right| - i\pi\Theta(k^2 - \omega^2) \right) \right). \quad (27)$$

One can see that the real part diverges at $\omega/k = 1$ and the imaginary part is linear with ω in the frequency region $\omega/k \leq 1$.

When $\nu > 0$, from (24)–(25) associated with R, θ in (23), one can see that the real and imaginary parts of the electric permittivity are smooth functions of ω without any frequency poles. Furthermore, the electric permittivity will gain a nonzero imaginary part both in the frequency region $\omega/k \leq 1$ and $\omega/k > 1$. In terms of the preceding discussion, one can see that compared to the collisionless case, the presence of collisions results in a remarkable change of ω -dependence of electric permittivity. A similar discussion can be applied to magnetic permeability. Therefore, one can expect that collisions might influence the refractive index through the collisional ϵ and μ_M .

We present n^2 and the Depine-Lakhtakia index n_{DL} in Figs. 3 and 4 respectively. When $\nu = 0$, n^2 and the Depine-Lakhtakia index n_{DL} change to the corresponding results in

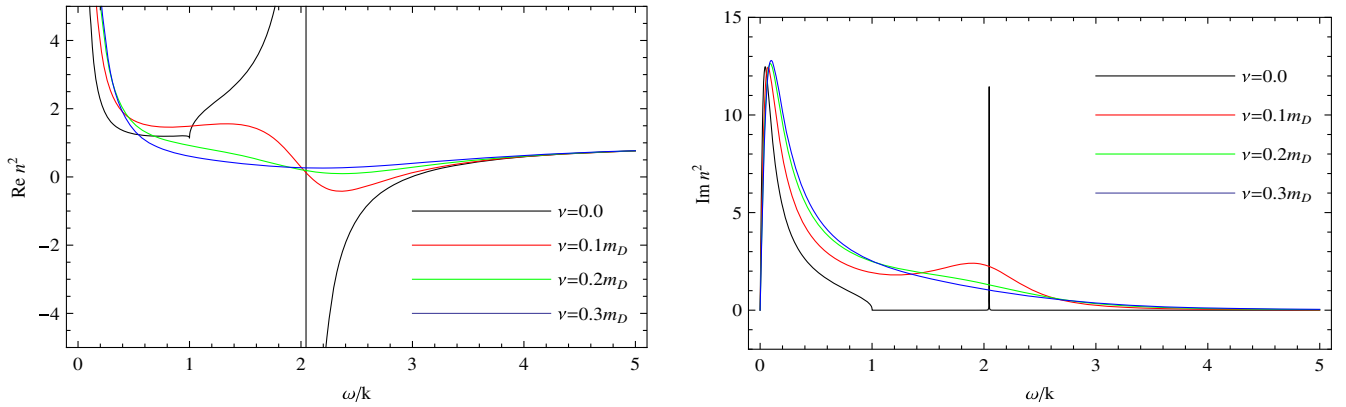


FIG. 3. n^2 for different collision rates in units of m_D . Left panel: The real parts. Right panel: The imaginary parts.

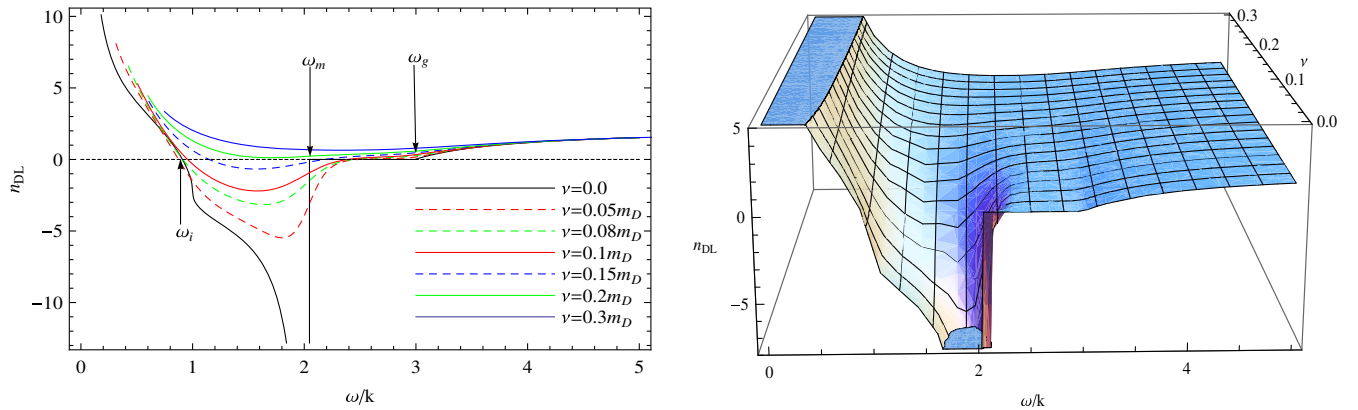


FIG. 4. Left panel: The Depine-Lakhtakia index n_{DL} for different collision rates. Right panel: Three-dimensional plot of n_{DL} as a function of ω and ν .

the HTLA [24,25], as shown by the black curves in Fig. 3 and in the left panel of Fig. 4. One can see that there are a frequency inflexion ω_i and a frequency pole ω_m for the Depine-Lakhtakia index n_{DL} . At the frequency pole ω_m of n_{DL} , the real and imaginary parts of n^2 are divergent. The frequency inflexion ω_i and the frequency pole ω_m of n_{DL} and n^2 are attributable to the frequency poles of the electric permittivity and magnetic permeability, which have already been elaborated in Ref. [25]. While for $\nu > 0$, the real and imaginary parts of n^2 and the Depine-Lakhtakia index n_{DL}

are smooth functions as shown by the colored curves in Fig. 3 and in the left panel of Fig. 4. According to the definitions of n^2 and the Depine-Lakhtakia index n_{DL} , one can see that compared to the collisionless case, the smooth ϵ and μ_M due to collisions result in analytically ω -dependent n^2 and the Depine-Lakhtakia index n_{DL} .

In the case of $\nu = 0$, as shown by the solid-black curve in the left panel in Fig. 4, n_{DL} becomes negative in some frequency range $\omega \in [\omega_i, \omega_m]$ with $\omega_i \approx k$, which implies a negative refractive index according to the preceding

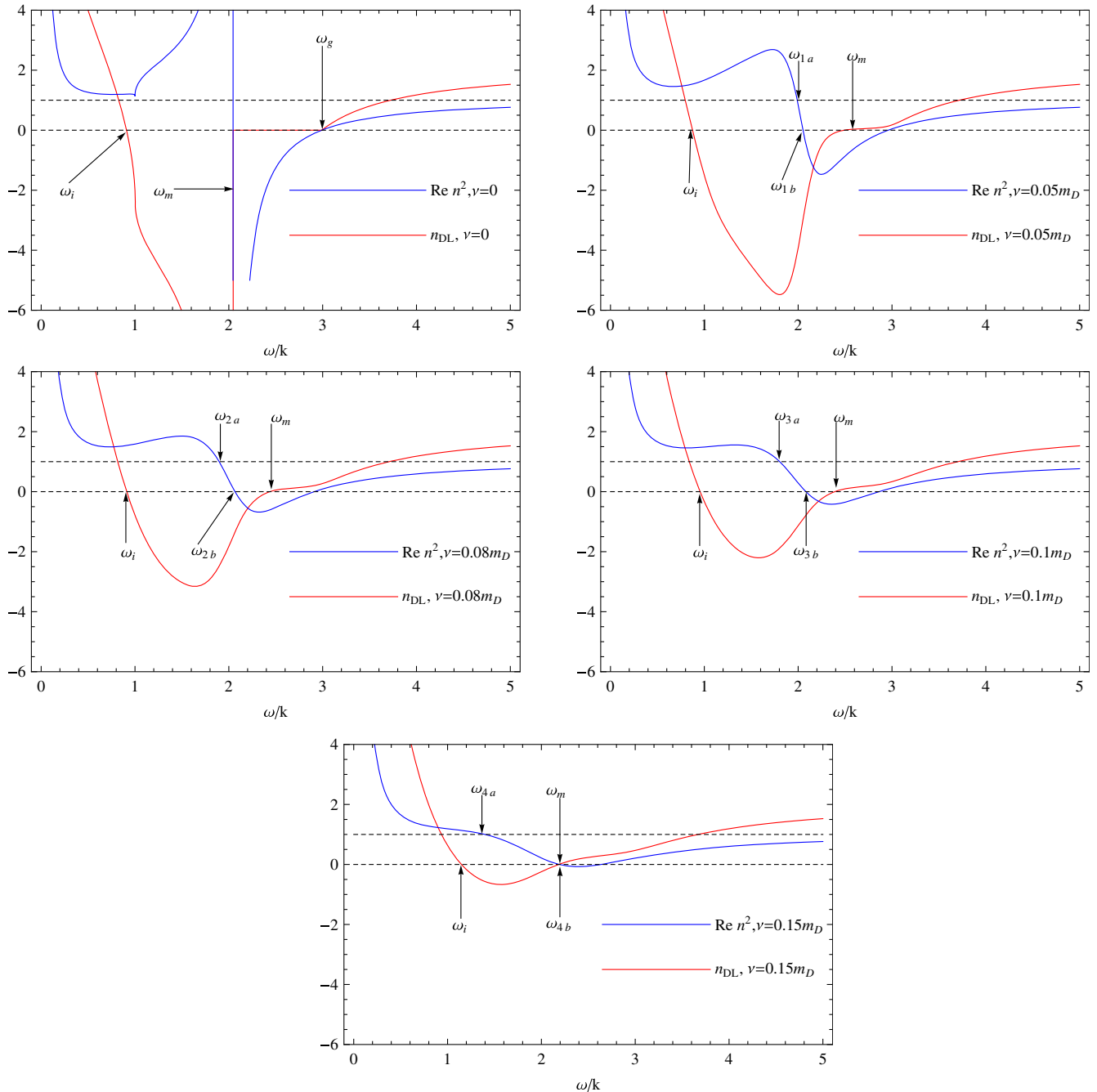


FIG. 5. The Depine-Lakhtakia index n_{DL} and the real part of n^2 for the different collision rates.

discussion in Sec. II. In addition, there is a frequency gap $\omega \in [\omega_m, \omega_g]$, in which the Depine-Lakhtakia index $n_{\text{DL}} = 0$ and $\text{Re} n^2 < 0$. In that frequency gap, light cannot propagate because the refraction index is pure imaginary and the electromagnetic wave is severely damped [24,25]. For a small ν , there exists some frequency range in which $n_{\text{DL}} < 0$. As ν increases, the frequency region for $n_{\text{DL}} < 0$ becomes narrower, as shown by the colored curves in the left panel of Fig. 4. It should be noted that in a previous paper, we have studied the viscous effect on the electromagnetic properties in QGP with the chromohydrodynamic approach. Our results show that the frequency range for the negative Depine-Lakhtakia index n_{DL} becomes wider as shear viscosity increases [25]. Collisions generally can drive the system to reach equilibrium, which is also responsible for dissipation. According to a very robust estimation $\eta \sim T^4/\nu$ [30], one can see that the results here qualitatively agree with those in the previous paper [25]. On the other hand, it is shown from the solid green curve in the left panel of Fig. 4 that there exists a critical collision rate around $0.2m_D$ above which $n_{\text{DL}} > 0$ for the whole frequency range, which indicates a normal refractive index. We also display the three-dimensional plot of the Depine-Lakhtakia index n_{DL} as a function of ω and ν in the right panel of Fig. 4, which might be helpful for understanding the refractive properties.

The criterion (11) $n_{\text{DL}} < 0$ has been widely used to judge the existence of negative refraction in a medium. However, Juan Liu *et al.* have argued that besides the condition $n_{\text{DL}} < 0$, the propagating mode should satisfy the dispersion relation $n^2\omega^2 = k^2$ simultaneously [24]. We present the $\text{Re} n^2$ and the Depine-Lakhtakia index n_{DL} in the same plots in Fig. 5, which may be helpful for understanding the existence of propagating modes for the dispersion relation $n^2\omega^2 = k^2$. In the case of $\nu = 0$, n_{DL} becomes negative in the frequency range $k < \omega < \omega_m$ [24]. It is displayed in Fig. 5 that $\text{Re} n^2 > 1$ in the same frequency region. There are no solutions for $n^2\omega^2 = k^2$ in that frequency range. Therefore, in the collisionless case, there are no propagation modes in the frequency region $k < \omega < \omega_m$ for a negative Depine-Lakhtakia index n_{DL} [24]. It is also argued that there exists strong dissipation in the frequency region for the negative Depine-Lakhtakia index in a strongly coupled system within the framework of AdS/CFT correspondence, propagation may dominate over dissipation only around $\omega \rightarrow 0$ [15].

However, for $\nu > 0$, as shown in Fig. 5, in the frequency regions $\omega_{1a} < \omega < \omega_{1b}$ for $\nu = 0.05m_D$, $\omega_{2a} < \omega < \omega_{2b}$ for $\nu = 0.08m_D$, $\omega_{3a} < \omega < \omega_{3b}$ for $\nu = 0.1m_D$, and $\omega_{4a} < \omega < \omega_{4b}$ for $\nu = 0.15m_D$, respectively, the Depine-Lakhtakia index n_{DL} will be negative. At the same time, $\omega_{1a}/k, \omega_{2a}/k, \omega_{3a}/k$, and ω_{4a}/k are larger than one and $0 < \text{Re} n^2 < 1$, the propagating modes may satisfy the dispersion relation $n^2\omega^2 = k^2$, which is another distinct aspect from the collisionless case. Some people have

investigated the collision effect on the dispersion relations based on the dielectric functions derived from the kinetic theory associated with the BGK collision term. Their results show that the finite collision rate ν will result in a spacelike dispersion ($\omega < k$) [34,35], which is responsible for the existence of a propagating mode satisfying $n^2\omega^2 = k^2$. Moreover, the frequency range in which $n_{\text{DL}} < 0$ and $0 < \text{Re} n^2 < 1$ becomes wider as the collision rate increases.

V. SUMMARY AND DISCUSSION

Within the framework of the kinetic theory associated with the BGK collisional term, we have derived the electric permittivity ϵ and the magnetic permeability μ_M of QGP. Our results show that in contrast with the collisionless case, collisional ϵ and μ_M are smooth functions of ω . Some algebraic analysis clearly demonstrates that compared to the collisionless case, the collisions dramatically change the ω -dependence of ϵ and μ_M . Based on the collisional ϵ and μ_M , we have studied the collision effect on the square of refractive index n^2 and the Depine-Lakhtakia index n_{DL} . The ω behavior of ϵ and μ_M modified by collisions is responsible for the analytic structure of the real and imaginary parts of n^2 and the Depine-Lakhtakia index n_{DL} . There is some frequency range in which the Depine-Lakhtakia index n_{DL} is negative for a small collision rate ν . However, the frequency range for $n_{\text{DL}} < 0$ becomes narrower as the collision rate ν increases. There exists a critical collision rate $\nu \sim 0.2m_D$ above which the Depine-Lakhtakia index n_{DL} is positive for the whole frequency region, which indicates a normal refractive index. In contrast to the collisionless case, there exists some frequency range in which $n_{\text{DL}} < 0$ and the propagating mode may satisfy the dispersion relation $n^2\omega^2 = k^2$ simultaneously, which implies that there may exist a negative refractive index.

Recently, some models have been proposed based on the refraction index to address diverse aspects of the phenomenology of ultrarelativistic heavy-ion collisions. A parton jet traveling through the hot medium produced in heavy-ion collisions may induce Cherenkov gluon radiation, which might contribute to the double peak structure of the experimental azimuthal dihadron correlation in the away side [50–52]. Some authors have investigated the photolike refraction of the gluon jet in the nonhomogeneous QGP produced in heavy-ion collisions, and they have argued that it might be a possible mechanism for the p_T -dependent away-side shape in central Au + Au collisions observed at the RHIC [53]. By phenomenologically modeling polarization and absorption mechanisms with a complex index of refraction, other investigations have shown that the radiative energy loss of an energetic charge can be substantially reduced in an absorptive medium [54,55], which might be helpful in understanding the jet-quenching phenomena in ultrarelativistic heavy-ion collisions at the RHIC and LHC.

In addition, some people have studied the effect of the QCD medium refraction on the elliptic flow and higher-order harmonics of prompt photons in high-energy heavy-ion collisions and found that refraction affects flow harmonics of prompt photons nontrivially [56]. Recently, some investigations have indicated that the refractive index in a medium under a strong magnetic field has two different physical propagating modes, i.e., birefringence, which will lead to a modification of the Hanbury-Brown-Twiss (HBT) interferometry of photons and the spectra of photons and dileptons in ultrarelativistic heavy-ion collisions [57,58]. Generally, negative refraction of light will lead to some special properties in a medium, such as modified refraction law, perfect lens, inverse Doppler and Cherenkov effect, inverse Snell's law, and so on. The negative refraction of QGP might lead to some novel effect on observables in ultrarelativistic heavy-ion collisions, which may be an interesting issue and needs a further comprehensive investigation.

ACKNOWLEDGMENTS

We are grateful to Yan-lin Lei for help numerical analysis in the early stage of work. Bing-feng Jiang is supported by the National Natural Science Foundation of China under Grants No. 11465007 and No. 11365008. De-fu Hou is supported by the Ministry of Science and Technology of the People's Republic of China under the "973" Project No. 2015CB856904(4) and by the National Natural Science Foundation of China under Grants No. 11375070, No. 11135011, and No. 11221504. Jia-rong Li is supported by the National Natural Science Foundation of China under Grant No. 11275082.

APPENDIX A: A DETAILED DERIVATION OF MAGNETIC PERMEABILITY IN EQ. (21)

As discussed in Appendix A in Ref. [25], in addition to the combination of electric permittivity ϵ and magnetic permeability μ_M , the following longitudinal and transverse dielectric functions ϵ_L , ϵ_T are usually used to describe the electromagnetic properties in plasma. The combination (ϵ_L, ϵ_T) can be related to ϵ and μ_M as follows:

$$\epsilon = \epsilon_L \quad (\text{A1})$$

$$\frac{1}{\mu_M} = 1 + \left(\frac{\omega^2}{k^2}\right) [\epsilon_L(\omega, k) - \epsilon_T(\omega, k)]. \quad (\text{A2})$$

In Refs. [34,37], the authors have derived the longitudinal and transverse dielectric functions by using the kinetic theory and the BGK-type collisional term

$$\epsilon_L(\omega, k) = 1 + \frac{m_D^2}{k^2} \left(1 - \frac{\omega + i\nu}{2k} \ln \frac{\omega + i\nu + k}{\omega + i\nu - k} \right) \times \left(1 - \frac{i\nu}{2k} \ln \frac{\omega + i\nu + k}{\omega + i\nu - k} \right)^{-1}, \quad (\text{A3})$$

$$\epsilon_T(\omega, k) = 1 - \frac{m_D^2}{2\omega(\omega + i\nu)} \left\{ 1 + \left[\frac{(\omega + i\nu)^2}{k^2} - 1 \right] \times \left(1 - \frac{\omega + i\nu}{2k} \ln \frac{\omega + i\nu + k}{\omega + i\nu - k} \right) \right\}. \quad (\text{A4})$$

We denote $z = \ln \frac{\omega + i\nu + k}{\omega + i\nu - k}$ and substitute it into the longitudinal and transverse dielectric functions. After some algebra, we can obtain

$$\epsilon_L(\omega, k) = 1 + \frac{m_D^2}{k^2} \frac{1 - \frac{\omega + i\nu}{2k} z}{1 - \frac{i\nu}{2k} z} = 1 + \frac{m_D^2}{k^2} \left\{ 1 - \frac{\omega z}{2k - i\nu z} \right\}, \quad (\text{A5})$$

$$\begin{aligned} \epsilon_T(\omega, k) &= 1 - \frac{m_D^2}{k^2} \left\{ \frac{k^2}{2\omega(\omega + i\nu)} \left[1 + \left(\frac{(\omega + i\nu)^2}{k^2} - 1 \right) \times \left(1 - \frac{\omega + i\nu}{2k} z \right) \right] \right\} \\ &= 1 - \frac{m_D^2}{k^2} \left\{ \frac{k^2}{2\omega(\omega + i\nu)} + \frac{(\omega + i\nu)^2 - k^2}{2\omega(\omega + i\nu)} \left(1 - \frac{\omega + i\nu}{2k} z \right) \right\} \\ &= 1 - \frac{m_D^2}{k^2} \left\{ \frac{2\omega + kz + i2\nu}{4\omega} - \frac{(\omega + i\nu)^2}{4\omega k} z \right\}. \end{aligned} \quad (\text{A6})$$

Substituting (A5) and (A6) into (A2),

$$\frac{1}{\mu_M} = 1 + \frac{\omega^2 m_D^2}{k^4} \left\{ 1 - \frac{\omega z}{2k - i\nu z} + \frac{2\omega + kz + i2\nu}{4\omega} - \frac{(\omega + i\nu)^2}{4\omega k} z \right\}; \quad (\text{A7})$$

therefore, we can finally obtain

$$\mu_M = \frac{1}{1 + \frac{\omega^2 m_D^2}{k^4} \left\{ 1 - \frac{\omega z}{2k - i\nu z} + \frac{2\omega + kz + i2\nu}{4\omega} - \frac{(\omega + i\nu)^2}{4\omega k} z \right\}}. \quad (\text{A8})$$

APPENDIX B: THE REAL AND IMAGINARY PARTS OF THE LOGARITHMIC FUNCTION $\ln \frac{\omega + k + i\nu}{\omega - k + i\nu}$

In the following, we will disentangle the real and imaginary parts from the logarithmic function $\ln \frac{\omega + k + i\nu}{\omega - k + i\nu} = a + bi$.

$$\ln \frac{\omega + k + i\nu}{\omega - k + i\nu} = \ln \frac{(\omega + k + i\nu)(\omega - k - i\nu)}{(\omega - k)^2 + \nu^2} = \ln \frac{\omega^2 - k^2 + \nu^2 - i2k\nu}{(\omega - k)^2 + \nu^2}. \quad (\text{B1})$$

After some algebra, we can obtain

$$\begin{aligned} \ln \frac{\omega + k + i\nu}{\omega - k + i\nu} &= \ln \left(\frac{\sqrt{(\omega^2 - k^2 + \nu^2)^2 + 4k^2\nu^2}}{(\omega - k)^2 + \nu^2} \left(\frac{(\omega^2 - k^2 + \nu^2)}{\sqrt{(\omega^2 - k^2 + \nu^2)^2 + 4k^2\nu^2}} - i \frac{2k\nu}{\sqrt{(\omega^2 - k^2 + \nu^2)^2 + 4k^2\nu^2}} \right) \right) \\ &= \ln(R(\cos \theta - i \sin \theta)) = \ln(Re^{-i\theta}) = \ln R + \ln e^{-i\theta} = \ln R - i\theta, \end{aligned} \quad (\text{B2})$$

with

$$\begin{aligned} a &= \ln R, \quad b = -\theta, \quad R = \frac{\sqrt{(\omega^2 - k^2 + \nu^2)^2 + 4k^2\nu^2}}{(\omega - k)^2 + \nu^2}, \\ \theta &= \arccos \frac{(\omega^2 - k^2 + \nu^2)}{\sqrt{(\omega^2 - k^2 + \nu^2)^2 + 4k^2\nu^2}}. \end{aligned} \quad (\text{B3})$$

Then, we can determine the logarithmic function in the limit of $\nu \rightarrow 0$:

$$\begin{aligned} \lim_{\nu \rightarrow 0} \ln \frac{\omega + k + i\nu}{\omega - k + i\nu} &= \lim_{\nu \rightarrow 0} \ln \frac{\sqrt{(\omega^2 - k^2 + \nu^2)^2 + 4k^2\nu^2}}{(\omega - k)^2 + \nu^2} \\ &\quad - i \lim_{\nu \rightarrow 0} \arccos \frac{(\omega^2 - k^2 + \nu^2)}{\sqrt{(\omega^2 - k^2 + \nu^2)^2 + 4k^2\nu^2}} \\ &= \ln \left| \frac{\omega + k}{\omega - k} \right| - i \arccos \frac{\omega^2 - k^2}{|\omega^2 - k^2|} \\ &= \ln \left| \frac{\omega + k}{\omega - k} \right| - i \begin{cases} 0, & \omega^2 > k^2 \\ \pi, & \omega^2 < k^2. \end{cases} \end{aligned} \quad (\text{B4})$$

We can express that result in a concise form with the step function Θ as

$$\ln \frac{\omega + k + i0^+}{\omega - k + i0^+} = \ln \left| \frac{\omega + k}{\omega - k} \right| - i\pi\Theta(k^2 - \omega^2). \quad (\text{B5})$$

APPENDIX C: THE REAL AND IMAGINARY PARTS OF THE COLLISIONAL ELECTRIC PERMITTIVITY IN EQS. (24) AND (25)

Substituting the disentangled the logarithmic function $\ln \frac{\omega+k+i\nu}{\omega-k+i\nu} = a + bi$ into the collisional electric permittivity Eq. (20),

$$\begin{aligned} \epsilon(\omega, k) &= 1 + \frac{m_D^2}{k^2} \left(1 - \frac{\omega + i\nu}{2k} \ln \frac{\omega + i\nu + k}{\omega + i\nu - k} \right) \\ &\quad \times \left(1 - \frac{i\nu}{2k} \ln \frac{\omega + i\nu + k}{\omega + i\nu - k} \right)^{-1}, \end{aligned} \quad (\text{C1})$$

one can obtain

$$\begin{aligned} \epsilon(\omega, k) &= 1 + \frac{m_D^2}{k^2} \cdot \frac{1 - \frac{\omega+i\nu}{2k} \cdot (a + ib)}{1 - \frac{i\nu}{2k} \cdot (a + ib)} \\ &= 1 + \frac{m_D^2}{k^2} \cdot \frac{(2k + b\nu - \omega a) - i(\omega b + a\nu)}{(2k + b\nu) - i a\nu} \\ &= 1 + \frac{m_D^2}{k^2} \cdot \frac{[(2k + b\nu - \omega a) - i(\omega b + a\nu)] \cdot [(2k + b\nu) + i a\nu]}{(2k + b\nu)^2 + (a\nu)^2} \\ &= 1 + \frac{m_D^2}{k^2} \cdot \left\{ 1 - \frac{2\omega k a}{4k^2 + b^2\nu^2 + 4kb\nu + a^2\nu^2} - i \frac{\omega\nu(a^2 + b^2) + 2\omega k b}{4k^2 + b^2\nu^2 + 4kb\nu + a^2\nu^2} \right\}. \end{aligned} \quad (\text{C2})$$

Therefore, the real and imaginary parts of the electric permittivity are expressed as

$$\text{Re}\epsilon_L(\omega, k) = 1 + \frac{m_D^2}{k^2} \cdot \left\{ 1 - \frac{2\omega k a}{4k^2 + b^2\nu^2 + 4kb\nu + a^2\nu^2} \right\} \quad (\text{C3})$$

and

$$\text{Im}\epsilon_L(\omega, k) = -\frac{m_D^2}{k^2} \cdot \frac{\omega\nu(a^2 + b^2) + 2\omega k b}{4k^2 + b^2\nu^2 + 4kb\nu + a^2\nu^2}. \quad (\text{C4})$$

In terms of $a = \ln R$, $b = -\theta$, One can arrive at

$$\text{Re}\epsilon_L(\omega, k) = 1 + \frac{m_D^2}{k^2} \cdot \left\{ 1 - \frac{2\omega k \ln R}{4k^2 + \nu^2(\theta^2 + \ln^2 R) - 4k\nu\theta} \right\}, \quad (\text{C5})$$

$$\text{Im}\epsilon_L(\omega, k) = -\frac{m_D^2}{k^2} \cdot \frac{\omega\nu(\theta^2 + \ln^2 R) - 2\omega k\theta}{4k^2 + \nu^2(\theta^2 + \ln^2 R) - 4k\nu\theta}, \quad (\text{C6})$$

where R, θ are defined in Eq. (B3) in Appendix B.

-
- [1] M. Gyulassy and L. McLerran, *Nucl. Phys.* **A750**, 30 (2005).
- [2] I. Arsene *et al.* (BRAHMS Collaboration), *Nucl. Phys.* **A757**, 1 (2005).
- [3] B. Back *et al.* (PHOBOS Collaboration), *Nucl. Phys.* **A757**, 28 (2005).
- [4] J. Adams *et al.* (STAR Collaboration), *Nucl. Phys.* **A757**, 102 (2005).
- [5] K. Adcox *et al.* (PHENIX Collaboration), *Nucl. Phys.* **A757**, 184 (2005).
- [6] K. Aamodt *et al.* (ALICE Collaboration), *Phys. Rev. Lett.* **105**, 252302 (2010).
- [7] G. Aad *et al.* (ATLAS Collaboration), *Phys. Rev. Lett.* **105**, 252303 (2010).
- [8] T. Lappi and L. McLerran, *Nucl. Phys.* **A772**, 200 (2006).
- [9] J. Liao and E. Shuryak, *Phys. Rev. C* **75**, 054907 (2007).
- [10] J. Liao and E. Shuryak, *Phys. Rev. Lett.* **101**, 162302 (2008).
- [11] D. Kharzeev, L. McLerran, and H. Warringa, *Nucl. Phys.* **A803**, 227 (2008).
- [12] K. Fukushima, D. Kharzeev, and H. Warringa, *Phys. Rev. D* **78**, 074033 (2008).
- [13] V. Skokov, A. Yu. Illarionov, and V. Toneev, *Int. J. Mod. Phys.* **A24**, 5925 (2009).
- [14] W.-t. Deng and X.-g. Huang, *Phys. Rev. C* **85**, 044907 (2012).
- [15] A. Amariti, D. Forcella, A. Mariotti, and G. Policastro, *J. High Energy Phys.* 04 (2011) 036.
- [16] A. Amariti, D. Forcella, A. Mariotti, G. Policastro, and M. Siani, *J. High Energy Phys.* 10 (2011) 104.
- [17] A. Amariti, D. Forcella, and A. Mariotti, *J. High Energy Phys.* 01 (2013) 105.
- [18] X.-h. Ge, K. Jo, and S.-J. Sin, *J. High Energy Phys.* 03 (2011) 104.
- [19] Xin Gao and H.-b. Zhang, *J. High Energy Phys.* 08 (2010) 075.
- [20] P. Phukon and T. Sarkar, *J. High Energy Phys.* 09 (2013) 102.
- [21] S. Mahapatra, P. Phukon, and T. Sarkar, *J. High Energy Phys.* 01 (2014) 135.
- [22] D. Forcella, A. Mezzalana, and D. Musso, *J. High Energy Phys.* 11 (2014) 153.
- [23] S. Mahapatra, *J. High Energy Phys.* 01 (2015) 148.
- [24] J. Liu, M. J. Luo, Q. Wang, and H.-j. Xu, *Phys. Rev. D* **84**, 125027 (2011).
- [25] B.-f. Jiang, De-fu Hou, J.-r. Li, and Y.-j. Gao, *Phys. Rev. D* **88**, 045014 (2013).
- [26] B.-f. Jiang and J.-r. Li, *Nucl. Phys.* **A847**, 268 (2010).
- [27] D. Forcella, J. Zaanen, D. Valentini, and D. van der Marel, *Phys. Rev. B* **90**, 035143 (2014).
- [28] C. A. A. de Carvalho, *Phys. Rev. D* **93**, 105005 (2016).
- [29] P. Bhatnagar, E. Gross, and M. Krook, *Phys. Rev.* **94**, 511 (1954).
- [30] S. Mrówczyński, in *Quark Gluon Plasma*, edited by R. C. Hwa (World Scientific, Singapore, 1990), Vol. 1, pp. 185–222.
- [31] A. Selikhov, *Phys. Lett. B* **268**, 263 (1991).
- [32] C. Manuel and S. Mrówczyński, *Phys. Rev. D* **68**, 094010 (2003).
- [33] M. Carrington and S. Mrówczyński, *Phys. Rev. D* **71**, 065007 (2005).
- [34] M. Carrington, T. Fugleberg, D. Pickering, and M. Thoma, *Can. J. Phys.* **82**, 671 (2004).
- [35] B. Schenke, M. Strickland, C. Greiner, and M. Thoma, *Phys. Rev. D* **73**, 125004 (2006).
- [36] M. Mandal and P. Roy, *Phys. Rev. D* **88**, 074013 (2013).
- [37] P. Chakraborty, M. Mustafa, R. Ray, and M. Thoma, *J. Phys. G* **34**, 2141 (2007).
- [38] H. A. Weldon, *Phys. Rev. D* **26**, 1394 (1982).
- [39] J. Meng and J.-r. Li, *Nucl. Phys.* **A730**, 97 (2004).
- [40] J. I. Kapusta, *Finite-Temperature Field Theory* (Cambridge University Press, Cambridge, England, 1989).
- [41] M. Le Bellac, *Thermal Field Theory* (Cambridge University Press, Cambridge, England, 1996).
- [42] V. G. Veselago, *Sov. Phys. Usp.* **10**, 509 (1968).
- [43] V. M. Agranovich and Yu. N. Gartstein, *Phys. Usp.* **49**, 1029 (2006).
- [44] S. A. Ramakrishna, *Rep. Prog. Phys.* **68**, 449 (2005).
- [45] J. B. Pendry, *Phys. Rev. Lett.* **85**, 3966 (2000).
- [46] D. R. Smith and N. Kroll, *Phys. Rev. Lett.* **85**, 2933 (2000).
- [47] M. W. McCall, A. Lakhtakia, and W. S. Weiglhofer, *Eur. J. Phys.* **23**, 353 (2002).
- [48] R. A. Depine and A. Lakhtakia, *Microwave Opt. Technol. Lett.* **41**, 315 (2004).
- [49] H.-T. Elze and U. Heinz, *Phys. Rep.* **183**, 81 (1989).
- [50] V. Koch, A. Majumder, and X.-N. Wang, *Phys. Rev. Lett.* **96**, 172302 (2006).
- [51] A. Majumder and X.-N. Wang, *Phys. Rev. C* **73**, 051901 (2006).
- [52] I. M. Dremin, *Nucl. Phys.* **A767**, 233 (2006).

- [53] H.-z. Zhang and En-ke Wang, [arXiv:0805.4058](#).
- [54] M. Bluhm, P. B. Gossiaux, and J. Aichelin, *Phys. Rev. Lett.* **107**, 265004 (2011).
- [55] M. Bluhm, P. B. Gossiaux, and J. Aichelin, *J. Phys. G* **38**, 124119 (2011).
- [56] A. Monnai, [arXiv:1408.1410](#).
- [57] K. Hattori and K. Itakura, *Ann. Phys. (N.Y.)* **330**, 23 (2013).
- [58] K. Hattori and K. Itakura, *Ann. Phys. (N.Y.)* **334**, 58 (2013).